Polymer 49 (2008) 3702–3708

Contents lists available at ScienceDirect

Polymer

journal homepage: www.elsevier.com/locate/polymer

Electrocopolymerization of aniline and *ortho*-phenylenediamine via facile negative shift of polyaniline redox peaks

Ali Parsa, Sulaiman Ab Ghani*

Pusat Pengajian Sains Kimia, Universiti Sains Malaysia, 11800 USM, Pulau Pinang, Malaysia

ARTICLE INFO

Article history:
Received 17 May 2008
Received in revised form 24 June 2008
Accepted 26 June 2008
Available online 2 July 2008

Keywords:
Electrocopolymerization
ortho-Phenylenediamine
Negative shift

ABSTRACT

Oxidative electropolymerization of aniline (Ani) in phosphoric acid (H_3PO_4) on composite 2B pencil graphite was accomplished using selected inorganic salts as supporting electrolytes. These salts determined the degree of conductivity of polyaniline (PAni) formed. The conductivity was in the order of $CaCl_2 > KCl > ZnCl_2 > ZnSO_4 > Ca_3(PO_4)_2$. The three pairs of redox peaks in the voltammogram of PAni formed in the presence of 0.06 M $Ca_3(PO_4)_2$ and 0.2 M $ZnSO_4$ have shifted 300 mV to the negative potential. The shifting of peaks is strongly influenced by type of anions' presence in the salts. However, the nature of the available cations had no significant effect. The negative shifts of redox peaks were exploited to facilitate the electrocopolymerization of Ani and *ortho*-phenylenediamine (*o*PD). The formation of the poly(Ani-*co*-*o*PD) was confirmed by the FTIR spectra.

1. Introduction

Although polyaniline (PAni) is one of the most important conducting polymers around, detailed study on its structure and properties only begun in the 1980s [1–7]. Generally, it is accepted that PAni is a redox polymer. Fig. 1a shows this blend where PAni has both the reduced benzenoid (B) unit (y) and the oxidized quinoid (Q) unit $(1-y)$ [8]. PAni may exist in several oxidation states, i.e. from the completely reduced leucoemeraldine (LE) state (Fig. 1b), where $1-y=0$, to the completely oxidized pernigraniline (PN) state, where $1-y=1$. The half-oxidized emeraldine base (EB) state, where $1-y=0.5$, is composed of an alternating sequence of two B units and one Q unit [9,10]. Even though each of these three states of PAni possesses quite interesting physical and chemical properties, they, actually, are insulators. However, the insulator blue EB may be conducting if it is doped with protic acids and become green protonated emeraldine (PE) or emeraldine salt (ES) with dc conductivity in the metallic region (ca. 1–5 S/cm) [11]. The later may also be obtained via a redox doping process of either its corresponding reduced LE or oxidized PN, by either a chemical or an electrochemical step in acid conditions (Fig. 1b). The deprotonation of ES revert this to EB.

PAni has a relatively good stability in air, even at elevated temperature, much better than that of other conducting polymers, e.g. polyacetylene [12]. But its intractable nature, such as insolubility, high brittleness, conductivity and electrochemical activity depend on medium's pH, acid-catalyzed oxidative degradation, etc. limits its application. Therefore, efforts have been made to modify PAni structurally to counter these problems. Among these, the copolymerization with some monomers is considered as the important method to improvise the properties of PAni [13–19]. The most significant aspect of copolymerization is that its properties can be regulated by adjusting the ratio of the monomers used [20,21].

The electrocopolymerization of Ani with other monomers is always difficult. In some cases it is impossible. This is due to the big difference of redox peak potentials (E_p) between Ani and the other monomers. The nearer the E_p of PAni to the E_p of the other monomer the better it is for the copolymerization to happen. Another equally important factor governing the quality of the copolymer obtained is the solvent used [22–27]. The solvent's physical and chemical properties can influence the redox coupled chemical reactions. The physical properties of solvent may affect both the rate and the equilibrium constants [28].

This work intends to investigate the characteristics of solvent H_3PO_4 and the corresponding supporting electrolytes, e.g. calcium chloride, potassium chloride, zinc chloride, calcium phosphate and zinc sulphate in the electrochemical synthesis of PAni on the surface of composite 2B pencil graphite. We have also reported on the influence of negative shifts of redox peaks on the electrocopolymerization of Ani with *o*PD. The morphology and structural analysis of this copolymer is examined using a scanning electron microscope (SEM) and FTIR.

* Corresponding author. Tel.: +60 4 653 4030; fax: +60 4 657 4854.
E-mail address: sag@usm.my (S. Ab Ghani).

0032-3861/$ – see front matter © 2008 Elsevier Ltd. All rights reserved.
doi:10.1016/j.polymer.2008.06.044

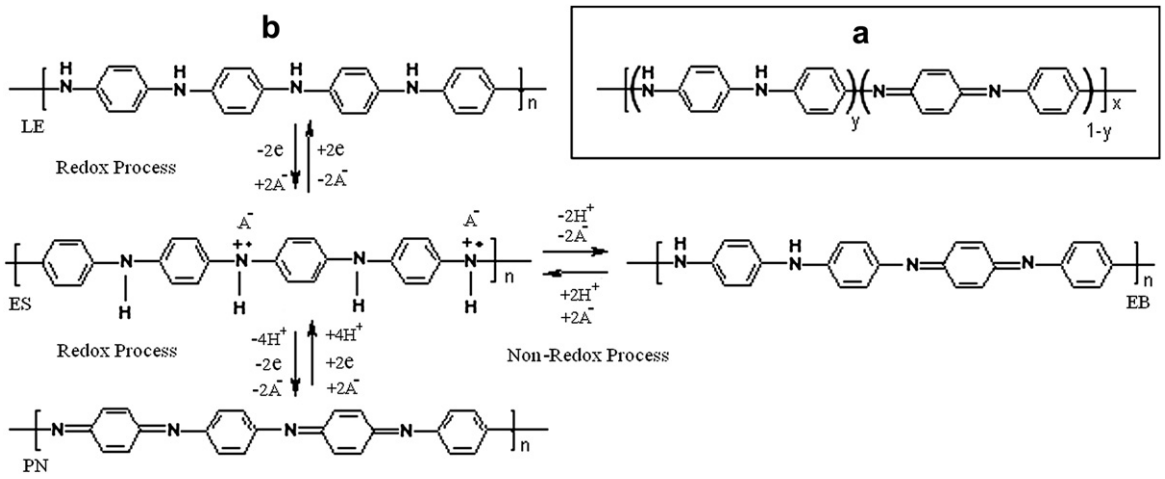

Fig. 1. (a) The general chemical structure of PAni that shows the average oxidation state $(1-y)$, (b) The chemical structures of the three normally found oxidation states of PAni and their transitions to the corresponding salt form (ES) either through a redox doping process or a non-redox doping process.

2. Experimental

2.1. Materials

Aniline (Sigma Chemicals, USA) was purified by distillation under a nitrogen atmosphere at reduced pressure. The resulting colorless liquid was kept in the dark at 5 °C. *ortho*-Phenylenediamine (*o*PD) and phosphoric acid (Sigma Chemicals, USA) were used as received. Inorganic salts, i.e. calcium chloride, potassium chloride, zinc chloride, calcium phosphate and zinc sulphate (Fluka Chemicals, Switzerland) were all of analytical grade. The *N*,*N*-dimethylformamide (DMF) (BDH Chemicals, UK) was used as received. Oxygen-free nitrogen (OFN) was obtained from Nissan-IOI (Malaysia). All aqueous solutions were freshly prepared using ultrapure water fro Milli Q plus (Millipore Corp., USA).

2.2. Equipment

Cyclic voltammetry was carried out over two different applied potential (E_{ap} vs. Ag/AgCl) ranges, i.e. −0.2 V to +1.0 V and −0.4 V to +1.0 V, using an electrochemical workstation Epsilon E2 (Bioanalytical System, USA) with scanning up to 21 cycles and rate 100 mV s^{-1}. A custom-made three-electrode cell was employed during synthesis and characterization of PAni. The composite 2B pencil graphite (Staedtler Lumograph, Germany) was used as working and counter electrodes against pseudo Ag/AgCl reference electrode. The conductivity was determined at room temperature using a custom-made four-probe kit in phase with a multimeter 197A (Keithley, USA). The structure of copolymer was determined by FTIR spectroscopy System 2000 (Perkin–Elmer, USA). The absorption spectra of PAni solution (in DMF) in the region of 400–2000 cm^{-1} were obtained using a UV–vis spectrophotometery V-500 (JASCO, Japan). The scanning electron microscopy (SEM) equipped with an Oxford INCA 400 energy dispersive X-ray (EDX) using a Leo Supra 50 VP field emission microanalysis system (Bucks, UK) was used to elucidate the morphology of the copolymer of Ani and *o*PD.

2.3. Procedure

The electrochemical syntheses were performed using 25 ml solution containing 50 mM monomer, 1 M H_3PO_4 and 0.5 M inorganic salts by sequentially sweeping the potential between the E_{ap} ranges mentioned at a scan rate 100 mV s^{-1} and under OFN atmosphere at 25 ± 2 °C.

3. Results and discussion

3.1. Electrochemical synthesis

Fig. 2 shows that for most cyclic voltammograms (CVs) during the first forward scan anodic peak O of the radical cation monomer is observed. However, on the reverse scan the cathodic peak is not always observed. This indicates that in the time-scale of the experiment (the sweep rate) the radical cation is rapidly consumed in a subsequent chemical reaction. Hence, it is an irreversible electrode process. Besides diminishing progressively the anodic peak shifts to a higher potential in the following scans. This indicates that the monomer is rapidly depleted in the vicinity of the electrode by changing to radical cation. The oxidation is limited to the diffusion of monomer from bulk solution [29]. It is also observed that current response at peak potential, +1.0 V, decreases as the cycles increase. This is due to the adsorption of PAni on the electrode. The PAni modified graphite is less conducting than the 2B pencil graphite [30].

However, with extended scanning the electrode process becomes more of quasi-reversible with increasing in oxidation and reduction currents [2]. Three pairs of redox peaks [31] are observed in the E_{ap} range of −0.4 V to +1.0 V. The first pair of redox peaks is in the potential range of −0.2 V to +0.3 V (denoted as O_3/R_3) that corresponds to the interconversion of LE to EB [32–34]. The second pair of redox peaks at potentials above +0.6 V (denoted as O_1/R_1) is due to oxidation of EB to PN (fully oxidized form) and vice-versa [32,33]. Those in the potential range from +0.3 V to +0.6 V (denoted as O_2/R_2) are attributed to oxidation of segments of PAni chain to benzoquinone (Bq) species, whose peak potentials are very close to one another and tend to disappear after several successive scans [6]. The pairs of O_3/R_3 and O_1/R_1 in 1 M H_3PO_4 containing inorganic salts are relatively sharper than those in 1 M H_3PO_4 without inorganic salts (Fig. 2a). The supporting electrolytes help in the mobility of radical cations to electrode surface for the formation of PAni. The green film of PAni appears soon after initiation of the polymerization. However, in solution without inorganic salt, the green film is not observed on the working electrode. Large shifting (∼300 mV) of three pairs of redox peaks in the negative direction in E_{ap} ranges of −0.4 V to +0.8 V is observed in Fig. 2b and c, but not in Fig. 2d–f. This shows that the shifting of the redox peaks depends strongly on the electrolyte composition. In Fig. 3 the redox peaks of PAni oxidation states in 1 M H_3PO_4 medium containing supporting electrolyte of $Ca_3(PO_4)_2$ (a) have shifted about 300 mV towards the negative direction compared to the $CaCl_2$ electrolyte (b).

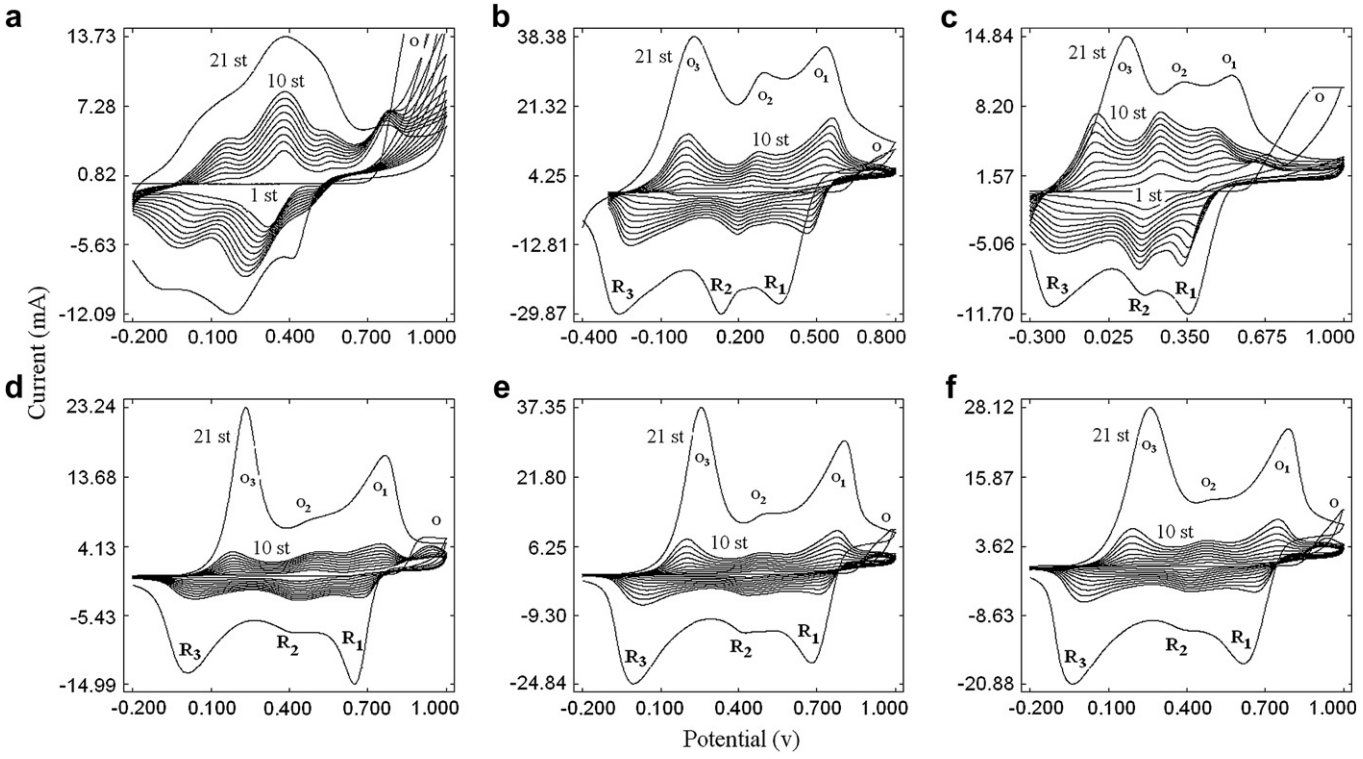

Fig. 2. The cyclic voltammograms obtained during electropolymerization of Ani in (a) 1 M H_3PO_4 and 1 M H_3PO_4 containing (b) 0.06 M $Ca_3(PO_4)_2$; (c) 0.2 M $ZnSO_4$; (d) 0.5 M $ZnCl_2$; (e) 0.5 M $CaCl_2$; and (f) 0.5 M KCl. The potential is cycled between −0.4 V and +1.0 V (vs. Ag/AgCl) at a scan rate of 100 mV s^{-1} for the 1st–21st cycle.

Exchanging the cations in the salts, regardless of their oxidation states, do not produce negative shifting. However, by exchanging the anions the negative shifts are observed. It is concluded that the shift depends on the anions present. This clearly shows that the solution's properties can influence the shift of redox peaks. Usually, solutions with good mass transport and limited ion pairing are used. This can be achieved if solvents have three major characteristics viz. (i) low donor number, (ii) low viscosity and (iii) high dielectric constant. The solvent polarity is usually expressed in terms of dielectric constant. Hence, solvents with low dielectric constants are non-polar, whilst those with high dielectric constants are polar. Therefore, a highly polar solvent is capable of enhancing the mass transport. The solvent medium may affect the monomer species in that it can become either as its donor or acceptor and also its electron transfer kinetics [28].

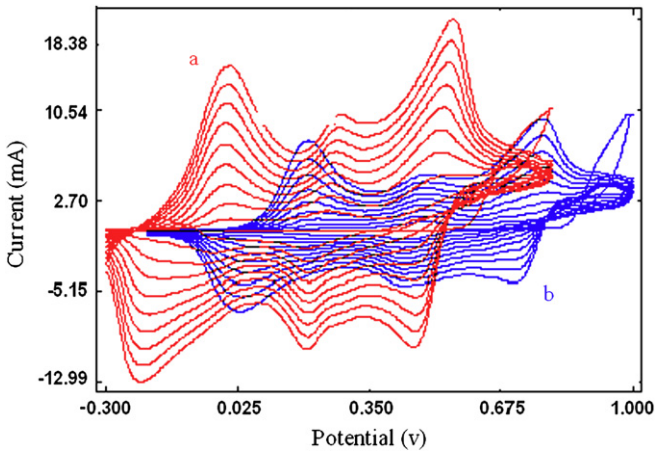

Fig. 3. The cyclic voltammograms obtained during electropolymerization of Ani in 1 M H_3PO_4 containing (a) 0.06 M $Ca_3(PO_4)_2$ and (b) 0.5 M $CaCl_2$.

3.2. Electrochemical response

In Fig. 4 the CVs at two different E_{ap} ranges (−0.2 V to +1.0 V and −0.3 V to +1.0 V) are scanned at 100 mV s^{-1} in a monomer-free H_3PO_4 solution (a) containing the inorganic salts (b–f). The first redox peaks O_3/R_3 correspond to the charge transfer from/to the PAni film [35,36]. The inorganic salt anion doping/dedoping of the PAni film compensate this charge transfer. The second redox peaks O_1/R_1 correspond to the protonation/deprotonation processes. During deprotonation the anion is expelled from the PAni film [37]. The small redox peaks of O_2/R_2 are probably due to degradation of quinoneimines structures [29].

3.3. Conductivity of PAni

Table 1 shows the list of conductivities of PAni formed in different supporting electrolytes. The conductivity of PAni is dependent on pH. It decreases significantly at pH higher than 3. The gradual increase of hydroxyl ion tends to initiate the formation of less soluble hydroxides of the electrolytes. Thus, this hinders the migration of cationic radicals to electrode surface. The conductivity is even lower in the medium without supporting. This study has illustrated that $CaCl_2$ as supporting electrolyte gives the best conductivity of PAni film. The conductivity of the polymer films decreases in the order of $CaCl_2 > KCl > ZnCl_2 > ZnSO_4 > Ca_3(PO_4)_2$. The influence of these salts on the electrical conductivity depends strongly on the anion present.

3.4. Structural analysis

The exact frequencies of FTIR assignments of PAni electrosynthesized in all media are shown in Table 2. The FTIR band spectra of PAni films are shown in Fig. 5. The absorption peaks at 1603 cm^{-1} and 1497 cm^{-1} can be attributed to the Q and B rings, respectively [38–40]. It has been reported [41] that the ratio of the

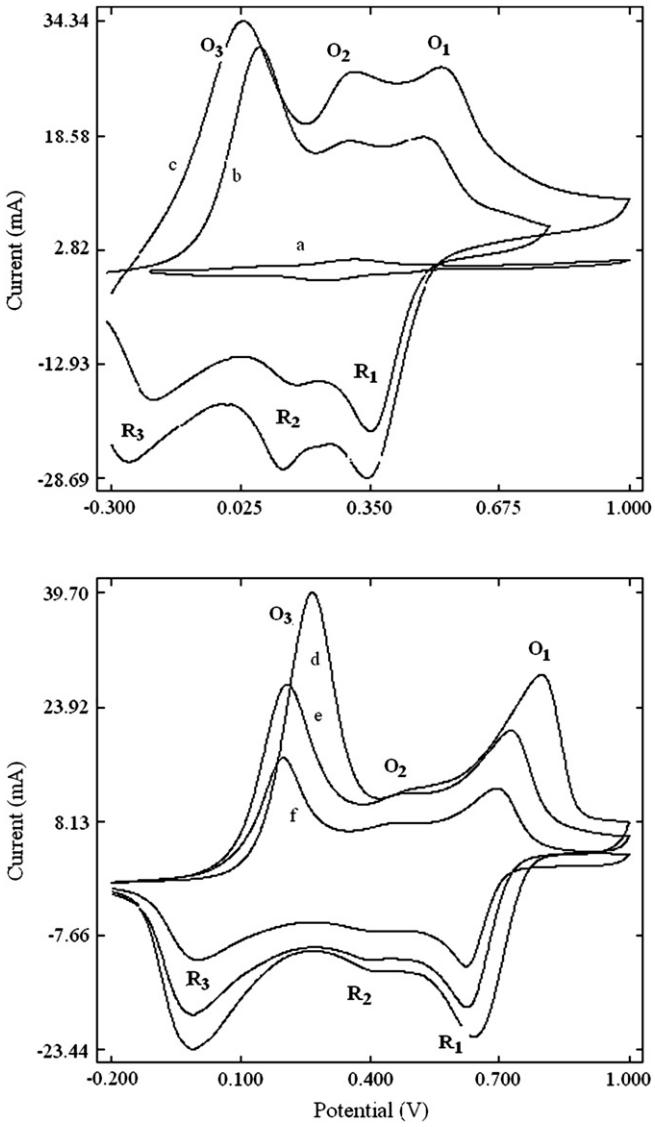

Fig. 4. Cyclic voltammetric responses of deposited PAni films in monomer-free solution at two different E_{ap} ranges (−0.2 V to +1.0 V and −0.3 V to +1.0 V) at a scan rate of 100 mV s^{-1} in (a) 1 M H_3PO_4, and 1 M H_3PO_4 containing (b) 0.06 M $Ca_3(PO_4)_2$, (c) 0.2 M $ZnSO_4$, (d) 0.5 M $ZnCl_2$, (e) 0.5 M $CaCl_2$, and (f) 0.5 M KCl.

intensity of bands of Q and B is a measure of the degree of oxidation of the PAni film. The ratio is 0 for the fully reduced form, 0.5–1 for the protoemeraldine form, 1 for the partially oxidized form and >1 for the fully oxidized form. Table 2 shows that the medium without inorganic salt has PAni in the oxidized form. Whereas, medium containing inorganic salts (Q/B ~ 1) has the partially oxidized PAni which, probably, is B as its most stable form. The infrared bands in the 1319 cm^{-1} and 1180 cm^{-1} are attributed to B and Q rings C–N stretching of emeraldine base (EB) [42]. However, in the present

Table 1
The conductivities of PAni formed in different media

	Media	Conductivity S/cm
a	1 M H_3PO_4	~10–6
b	1 M H_3PO_4 + 0.5 M $CaCl_2$	~3
c	1 M H_3PO_4 + 0.5 M KCl	~2.7
d	1 M H_3PO_4 + 0.5 M $ZnCl_2$	~2.05
e	1 M H_3PO_4 + 0.06 M $Ca_3(PO_4)_2$	~0.08
f	1 M H_3PO_4 + 0.2 M $ZnSO_4$	~0.18

Table 2
The FTIR absorption bands

	Media					
	1 M H_3PO_4 + 0.5 M				1 M H_3PO_4	
	1 M H_3PO_4	$CaCl_2$	KCl	$ZnCl_2$	0.06 M $Ca_3(PO_4)_2$	0.2 M $ZnSO_4$
Quinoid(Q)	1614	1603	1618	1618	1619	1640
Benzenoid(B)	1491	1497	1501	1498	1498	1498
CN Stretching	1240	1237	1257	1248	1238	1227
	1308	1314	1306	1311	1311	1311
CH in plan bending	1149	1158	1155	1155	1155	1158
CH out-of-plan bending	818	819	818	818	816	820
Ratio Q/B	~1.5	~1	~1	~1	~1	~1

study the bands at 1314 cm^{-1} and 1237 cm^{-1} are for emeraldine salt (ES) [43,44]. The bands at 1158 cm^{-1} and 819 cm^{-1} are assigned to in-plane and out-of-plane C–H bending motions of the aromatic rings, respectively [43]. The characteristic band of the conducting protonated form of PAni is reported to occur at 1252 cm^{-1} [45]. In the current study it is, however, observed that this band occurs at about 1310 cm^{-1}. Thus, these IR absorption spectra show that the obtained PAni is actually in the ES form. The intensity of the Q-ring stretching vibration is higher than that of the B band (Fig. 5a). Hence, the existence of a higher percentage of Q structure units in the polymeric chain is expected. This also means that in ionic liquid

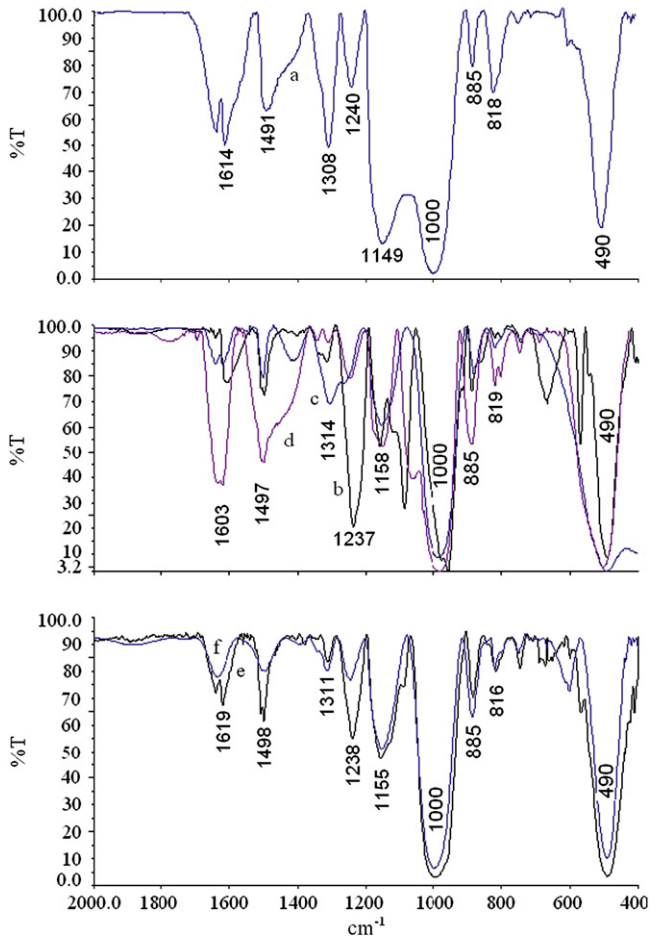

Fig. 5. Baseline corrected FTIR spectra (2000–400 cm^{-1} region) of PAni electropolymerized from (a) 1 M H_3PO_4, and 1 M H_3PO_4 containing (b) 0.5 M $CaCl_2$, (c) 0.5 M KCl, (d) 0.5 M $ZnCl_2$, (e) 0.06 M $Ca_3(PO_4)_2$ and (f) 0.2 M $ZnSO_4$.

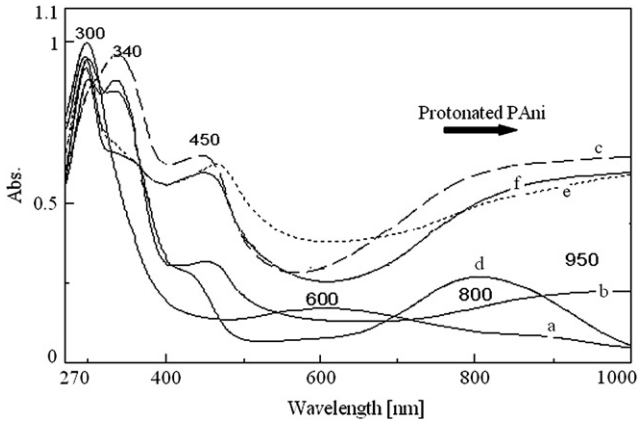

Fig. 6. UV–vis spectra of PAni solution in DMF. The polymers were deposited from 50 mM Ani in (a) 1 M H_3PO_4 and 1 M H_3PO_4 containing (b) 0.5 M $CaCl_2$, (c) 0.5 M KCl, (d) 0.5 M $ZnCl_2$, (e) 0.2 M $ZnSO_4$ and (f) 0.06 M $Ca_3(PO_4)_2$.

media, PAni may have a small amount of non-conducting EB and/or PN formed, i.e. more Q structures in the polymer backbone. A broad band at 1000 cm^{-1} corresponds to the phosphate anion [46,47]. The vibrational bands located in the range of 1050–960 cm^{-1} and at 604 cm^{-1}, 567 cm^{-1} and 490 cm^{-1} are associated with the $(PO_4)^{3-}$ groups. Also the band at 885 cm^{-1} is characteristic of $(HPO_4)^{2-}$ [48].

The UV–vis absorption intensity of the polymeric solutions can be used to study on the availability of mid-gap state caused by charge transfer. In Fig. 6a, the spectrum of PAni (medium 1 M H_3PO_4) solution in DMF is dominated by two absorption peaks, 300 nm and 600 nm [49]. These bands are attributed to $\pi \rightarrow \pi^*$ and $n \rightarrow \pi^*$ electronic transitions in B and Q, respectively, in the EB (middle oxidation state) of PAni [2,3,43]. In others (medium: 1 M H_3PO_4 containing inorganic salts), three absorption peaks at 340 nm, 450 nm and 800 nm are prominent. The existence of these peaks has also been reported elsewhere [34,50]. The broad peak at 340 nm is the $\pi \rightarrow \pi^*$ transition in the B ring of the reduced, non-conducting LE [40,51,52]. It has also been reported [53,54] that the cationic radical of aromatic amines in aqueous solutions has a characteristic absorption peak at 450 nm. The peaks at about 450 nm and 800 nm are for the ES phase of PAni and can be assigned to the polaronic and bipolaronic transitions of the Ani unit [55,56]. The transition of the excitonic (at 600 nm) to bipolaronic (at 800 nm) characterizes an increase in the electronic mobility [34]. It is reported that the absorbance at 800 nm may also be due to localized polarons in PAni [54,57]. During electropolymerization of Ani, the intensity of the absorption bands from the localized polarons decreases. On the other hand, the intensity of free charge carrier tail is associated with the delocalized polaron band (at 1000 nm) which increases steadily into the near-IR region [54,55,58]. However, these absorption bands, i.e. at 450 nm and 800–1000 nm, diminish when conductivity decreases.

3.5. Electrocopolymerization of oPD and Ani

Fig. 7 shows the CVs (a) for the growth of poly *ortho*-phenylenediamine (PoPD) from a 50 mM *o*PD solution in 1 M H_3PO_4 containing 0.5 M $CaCl_2$. The voltammogram is cycled between E_{ap} range of −0.6 V and +0.9 V (vs. Ag/AgCl) at a scan rate of 100 mV s^{-1} and up to 10 cycles. During the first positive sweep, a large anodic current is observed and an oxidation peak (denoted O) appears at around +0.660 V. This is attributed to the oxidation of the monomers on the electrode surface. However, on the reverse scan, cathodic, the reduction peak is not always observed. Due to the growth of polymer film on the electrode surface the oxidation peak progressively diminishes and shifts to a lower potential on the

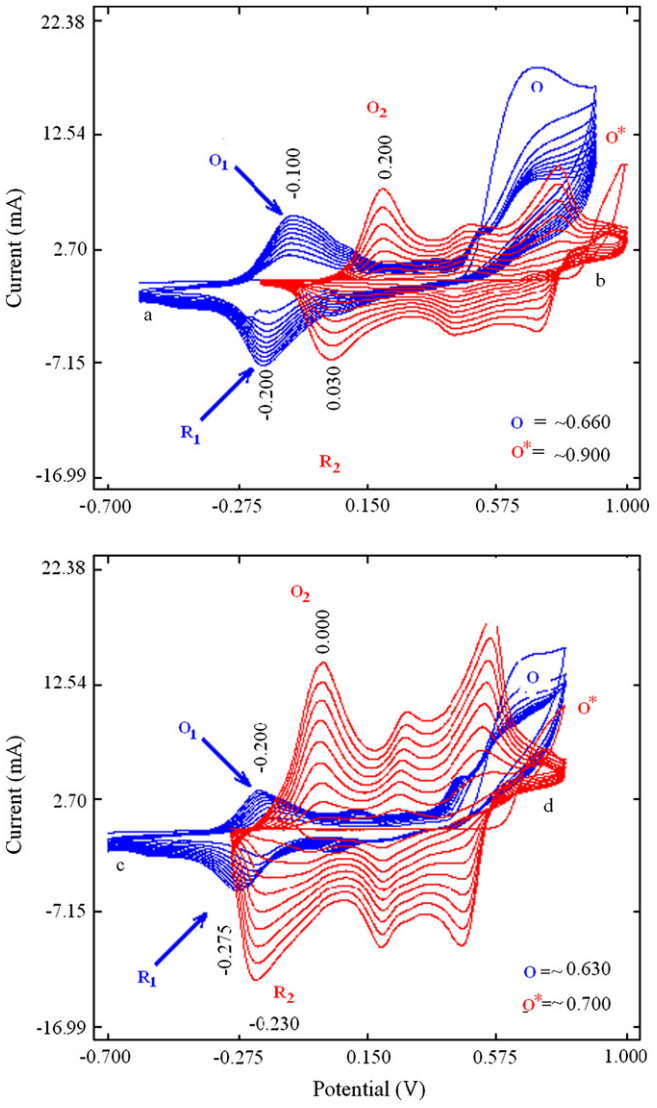

Fig. 7. The CVs for the growth of PoPD from a 50 mM *o*PD solution in 1 M H_3PO_4 containing (a) 0.5 M $CaCl_2$ and (c) 0.06 M $Ca_3(PO_4)_2$. The voltammogram is cycled between E_{ap} −0.7 V and +0.9 V (vs. Ag/AgCl), scan rate of 100 mV s^{-1} and up to 10 cycles. The (b) and (d) are CVs for the growth of PAni from a 50 mM Ani solution in 1 M H_3PO_4 containing 0.5 M $CaCl_2$ and 0.06 M $Ca_3(PO_4)_2$, respectively. The voltammogram is cycled between E_{ap} −0.4 V and +1.0 V (vs. Ag/AgCl), scan rate 100 mV s^{-1} and up to 10 cycles.

subsequent scans. In the following negative sweep, main reduction peak, at around −0.200 V (denoted R_1) is observed. Correspondingly, there is an anodic peak at around −0.100 V (denoted, O_1) in the subsequent positive sweeps. During the electropolymerization process, the electrolyte becomes light brown in color which is likely due to formation of soluble oligomers during the oxidation process. It is reported [59] that the oligomers are oxidized at a potential lower than that of the monomers. The CVs (c) shows the first 10 cycles of electropolymerization of *o*PD in the E_{ap} range between −0.700 V and +0.800 V in 1 M H_3PO_4 containing 0.06 M $Ca_3(PO_4)_2$. The pairs of redox peaks in the range from −0.7 V to +0.8 V have shifted in a negative direction (50–100 mV) in relation to CVs (a). The CVs (b) and (d) show the growth of PAni from a 50 mM Ani solution in 1 M H_3PO_4 containing 0.5 M $CaCl_2$ and 0.06 M $Ca_3(PO_4)_2$, respectively. The voltammogram is cycled between E_{ap} of −0.4 V and +1.0 V (vs. Ag/AgCl) at a scan rate 100 mV s^{-1} and up to 10 cycles. The formation of Ani radical cations in (b) proceeds at ca. 0.9 V in the first cycle (denoted as O^*) indicating that the

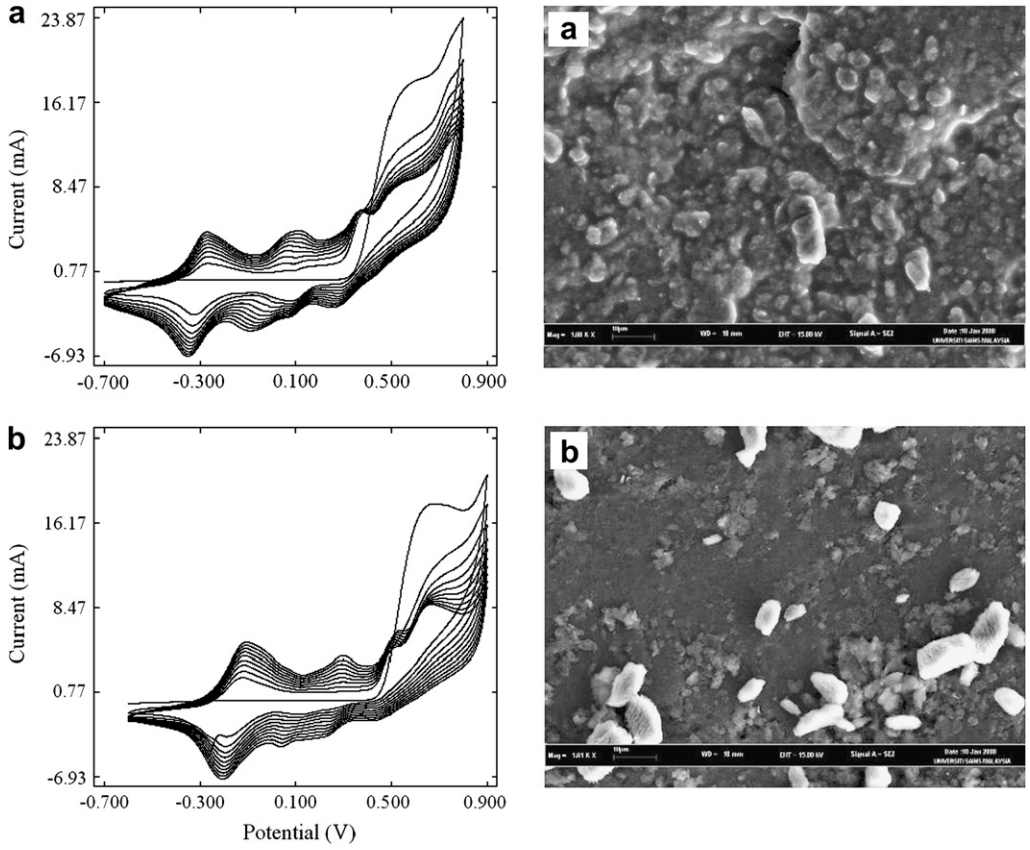

Fig. 8. The CVs and SEM images of copolymerization of 50 mM Ani solution and 50 mM *o*PD solution in 1 M H_3PO_4 containing (a) 0.06 M $Ca_3(PO_4)_2$ and (b) 0.5 M $CaCl_2$. The voltammogram is cycled between E_{ap} −0.7 V and +0.9 V (vs. Ag/AgCl), scan rate of 100 mV s^{-1} and up to 10 cycles.

electrodeposition of PAni has resulted on the electrode surface. However, in the *o*PD case (a), the formation of *o*PD radical cations has proceeded at a lesser potentials (0.66 V, denoted O) as compared to Ani. Thus, the P*o*PD is more easily deposited on the electrode surface. On the other hand, when $CaCl_2$ is the supporting electrolyte, redox peak couples of PAni and P*o*PD are far from each other. In the electrocopolymerization of Ani and *o*PD using $CaCl_2$ as supporting electrolyte the deposition of P*o*PD should occur first on the electrode surface. The resultant copolymers should then exhibit more towards P*o*PD-like nature.

The CV and SEM image of copolymerization of Ani and *o*PD in 1 M H_3PO_4 containing 0.06 M $Ca_3(PO_4)_2$ are shown in Fig. 8a. The CVs and SEM image of copolymerization of Ani and *o*PD in 1 M H_3PO_4 containing 0.5 M $CaCl_2$ (Fig. 8b) show that the CVs are very much similar to that in the *o*PD case, (a) in Fig. 7. Also the oxidation current of Ani becomes almost inconspicuous and the SEM image appears not quite homogeneous. However, when $Ca_3(PO_4)_2$ is used as supporting electrolyte, (c) and (d) in Fig. 7, the redox peak couples of PAni and P*o*PD are very near to each other. This implies that the polymer deposit consists of similar moieties of P*o*PD and PAni.

Further evidence on the formation of the copolymer is obtained with FTIR spectroscopy (Fig. 9). The spectra show absorption bands of the P*o*PD in 1 M H_3PO_4 containing (a) $Ca_3(PO_4)_2$ and (b) $CaCl_2$. The bands at 1640 cm^{-1} and 1406 cm^{-1} are assigned to C=C stretching vibrations of Q and B rings. The bands at 1319 cm^{-1} and 1284 cm^{-1} are assigned to C–N stretching vibrations of the Q and B rings. The band at 820 cm^{-1} is the C–H out-of-plane bending motion of the 1,2,4,5-tetrasubstituted benzene nuclei of phenazine units. The bands at 1064 cm^{-1} and 930 cm^{-1} are due to in-plane and out-of-plane bending motion of the C–H of the 1,2,4-tri substituted benzene rings indicating the presence of open rings in the phenazine units [60]. The bands at 1008 cm^{-1} and 578 cm^{-1} are assigned to a C–H in-plane and out-of-plane bending vibration, respectively [61].

Fig. 10 shows variations in the intensity FTIR spectra of the main bands of the copolymers. The band at 1634–1618 cm^{-1} indicates existence *o*PD in the copolymer. The appearance of the bands at 1068–1064 cm^{-1}, 884 cm^{-1} and 850 cm^{-1} suggests the presence of phenazine-like cyclic structures in the copolymer backbone. These cyclic structures in the copolymer could either be due to the presence of P*o*PD blocks or may result from the cyclic formation of the adjacent *o*PD and Ani unit in the copolymeric chain. The

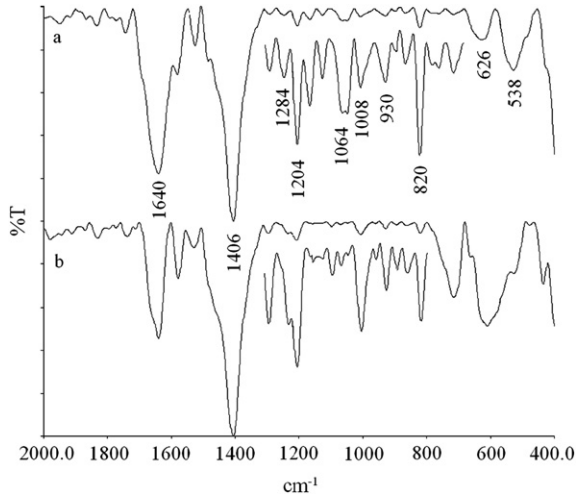

Fig. 9. Baseline corrected FTIR spectra (2000–400 cm^{-1} region) of P*o*PD electropolymerized in 1 M H_3PO_4 containing (a) 0.06 M $Ca_3(PO_4)_2$ and (b) 0.5 M $CaCl_2$.

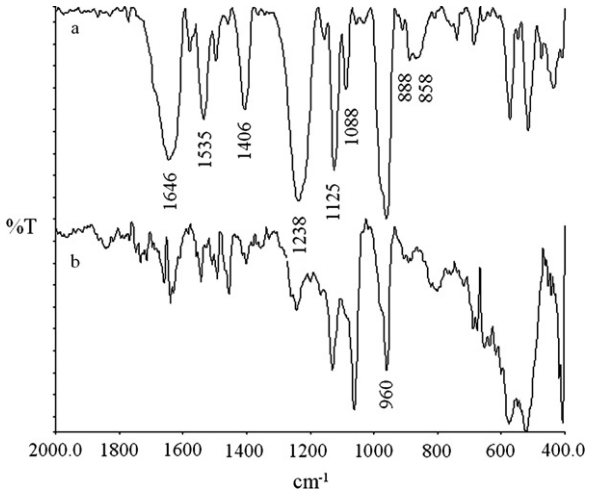

Fig. 10. Baseline corrected FTIR spectra (2000–400 cm^{-1} region) of copolymer of Ani and *o*PD in 1 M H_3PO_4 containing (a) 0.06 M $Ca_3(PO_4)_2$ and (b) 0.5 M $CaCl_2$.

presence of above bands in the copolymer synthesized in 1 M H_3PO_4 containing $Ca_3(PO_4)_2$ (a) is obvious from the one synthesized in 1 M H_3PO_4 containing $CaCl_2$ (b).

4. Conclusions

This study has illustrated that by using an H_3PO_4 (polar) medium containing $Ca_3(PO_4)_2$ a considerable shift of the PAni redox peaks towards negative potentials is obtained. The nearer the redox peaks of PAni to redox peaks of other monomers the easier it becomes to copolymerize. This is an indication that a more feasible synthesis of various Ani copolymers can be obtained. This study also indicates that the copolymerization depends on the anions present in phosphoric acid medium.

Both FTIR and UV–vis spectra confirm that the resulting PAni is in its conducting state. The FTIR band intensity ratio of Q/B indicates that PAni film is in partially oxidized state. The ratio of Q/B vibrations suggests that PAni is in emeraldine salt form. In the UV–vis region a pure PAni, however, has a broad absorption peak beyond 750 nm which is associated with the oxidation of the polymer, giving rise to the polaronic states within the band gap. The electrosynthesis of poly(Ani-*co*-*o*PD) in 1 M H_3PO_4 containing $Ca_3(PO_4)_2$ is confirmed by the FTIR spectra and SEM image.

Acknowledgment

This work is supported by the Ministry of Higher Education, Malaysia under Research University (RU) Grant no. 1001/PKIMIA/811044.

References

[1] Diaz AF, Logan JA. J Electroanal Chem 1980;111:111–4.
[2] Huang WS, Humphrey BD, MacDiarmid AG. J Chem Soc Faraday Trans 1 1986;82:2385–400.
[3] Lj Duic, Mandic Z, Kovacicek F. J Polym Sci Part A Polym Chem 1994;32:105–11.
[4] Inzelt G, Horanyi G. Electrochim Acta 1990;35:27–34.
[5] Genies EM, Lapkowski M, Penneau JF. J Electroanal Chem 1988;249:97–107.
[6] Stilwell DE, Park SM. J Electrochem Soc 1988;135:2497–502.
[7] Stilwell DE, Park SM. J Electrochem Soc 1988;135:2491–6.
[8] Wei D, Lindfors T, Kvarnstrom C, Kronberg L, Sjoholm R, Ivaska A. J Electroanal Chem 2005;575:19–26.
[9] MacDiarmid AG, Chiang JC, Richter AF, Epstein AJ. Synth Met 1987;18:285–90.
[10] Inzelt G. Electrochim Acta 2000;45:3865–76.
[11] Chiang JC, MacDiarmid AG. Synth Met 1986;13:193–205.
[12] Prokeš J, Stejskal J. Polym Degrad Stab 2004;86:187–95.
[13] Conklin JA, Huang SC, Huang SM, Wen T, Kaner RB. Macromolecules 1995;28:6522–7.
[14] Pandey SS, Annapoorni S, Malhotra BD. Macromolecules 1993;26:3190–3.
[15] Chan HSO, Ng SC, Sim WS, Tan KL, Tan BTG. Macromolecules 1992;25:6029–34.
[16] Anbarasan R, Jayaseharan J, Gopalan A. J Appl Polym Sci 2002;85:2317–26.
[17] Mazeikiene R, Malinauskas A. Synth Met 1998;92:259–63.
[18] Tu X, Xie Q, Xiang C, Zhang Y, Yao S. J Phys Chem B 2005;109:4053–63.
[19] Malinauskas A, Bron M, Holze R. Synth Met 1998;92:127–37.
[20] Wei Y, Hariharan R, Patel SA. Macromolecules 1990;23:758–64.
[21] Bilal S, Holze R. Electrochim Acta 2007;52:5346–56.
[22] Tagowska M, Pałys B, Jackowska K. Synth Met 2004;142:223–9.
[23] Huang K, Wan M. Chem Mater 2002;14:3486–92.
[24] Huang J, Kaner RB. J Am Chem Soc 2004;126:851–5.
[25] Athawale AA, Deore BA, Kulkarni MV. Mater Chem Phys 1999;60:262–7.
[26] Mandic Z, Duic Lj, Kovacicek F. Electrochim Acta 1997;42:1389–402.
[27] Mohamoud MA, Hillman AR. Electrochim Acta 2007;53:1206–16.
[28] Izutsu K. Electrochemistry in nonaqueous solutions. New York: John Wiley VCH; 2002. p. 20.
[29] Barrios EM, Mujica GA, Velasquez CL, Martinez Y. J Electroanal Chem 2006;586:128–35.
[30] Choi SJ, Park SM. J Electrochem Soc 2002;149:E26–34.
[31] Eftekhari A, Afshani R. J Polym Sci Part A Polym Chem 2006;44:3304–11.
[32] Macdiamid AG, Epstein AJ. Faraday Discuss Chem Soc 1989;88:317–32.
[33] Ray A, Richter AF, Macdiarmid AG, Epstein AJ. Synth Met 1989;29:151–6.
[34] Motheo AJ, Pantoja MF, Venancio EC. Solid State Ionics 2004;171:91–8.
[35] Stilwell DE, Park SM. J Electrochem Soc 1988;135:2254–62.
[36] Ulgut B, Zhao Y, Grose JE, Ralph DC, Abruna HD. Langmuir 2006;22:4433–7.
[37] Orata D, Buttry DA. J Am Chem Soc 1987;109:3574–81.
[38] Kan J, Lv R, Zhang S. Synth Met 2004;145:37–42.
[39] Sbaite P, Huerta-Vilca D, Barbero C, Miras MC, Motheo AJ. Eur Polym J 2004;40:1445–50.
[40] Yagan A, Pekmez NO, Yıldız A. Electrochim Acta 2006;51:2949–55.
[41] Shah K, Iroh J. Synth Met 2002;132:35–41.
[42] Virji S, Kaner RB, Weiller BH. Chem Mater 2005;17:1256–60.
[43] Lesiak B, Jablonski A, Zemek J, Trchova M, Stejskal J. Langmuir 2000;16:1415–23.
[44] Trchova M, Sedenkova I, Tobolkova E, Stejskal J. Polym Degrad Stab 2004;86:179–85.
[45] Wei D, Kvarnstrom C, Lindfors T, Ivaska A. Electrochem Commun 2006;8:1563–6.
[46] Weber M, Nart FC. Electrochim Acta 1996;41:653–9.
[47] Weber M, Moraes IR, Motheo AJ, Nart FC. Colloids Surf A 1998;134:103–11.
[48] Zhai YQ, Li KZ, Li HJ, Wang C, Liu H. Mater Chem Phys 2007;106:22–6.
[49] Gupta V, Miura N. Mater Lett 2006;60:1466–9.
[50] Ram MK, Sarkar N, Ding H, Nicolini C. Synth Met 2001;123:197–206.
[51] Sainz R, Benito AM, Martinez MT, Galindo JF, Sotres J, Baro AM, et al. Adv Mater 2005;17:278–81.
[52] Ozcicek NP, Pekmez K, Holze R, Yıldız A. J Appl Polym Sci 2003;90:3417–23.
[53] Wen TC, Sivakumar C, Gopalan A. Electrochim Acta 2001;46:1071–85.
[54] Wei D, Kvarnström C, Lindfors T, Kronberg L, Sjöholm R, Ivaska A. Synth Met 2006;156:541–8.
[55] Furukawa Y. J Phys Chem 1996;100:15644–53.
[56] Sankarasubramanian M, Santhosh P, Gopalan A, Vasudevan T. J Macromol Sci Part A 2004;41:1285–301.
[57] Epstein AJ, Ginder JM, Zuo F, Bigelow RW, Woo HS, Tanner DB, et al. Synth Met 1987;18:303–9.
[58] Furukawa Y. Vib Spectrosc 1999;19:77–83.
[59] Barbero C, Silber JJ, Sereno L. J Electroanal Chem 1989;263:333–52.
[60] Huang MR, Li XG, Duan W. Polym Int 2005;54:70–82.
[61] Murugesan R, Subramanian E. Mater Chem Phys 2003;80:731–9.